細胞周期依存的な先端成長に異常を示す出芽酵母非必須遺伝子破壊株の網羅的解析

渡邉 街香

東京大学大学院新領域創成科学研究科

先端生命科学専攻

2006

修士論文

Comprehensive and Quantitative Analysis of Yeast Deletion Mutants Defective in Cell Cycle-Dependent Polarized Cell Growth

Machika Watanabe

Department of Integrated Biosciences

Graduate School of Frontier Sciences

University of Tokyo

2006

Master Thesis

ACKNOWLEDGEMENT

I wish to express my deepest appreciation to Professor Yoshikazu Ohya for his constant supervision, excellent advice, valuable discussion and patient encouragement through the course of this study.

I also express my appreciation to Assistant professor Kintake Sonoike for his discussion and encouragement throughout this study.

I am grateful to Professor Shinichi Morishita for his insightful suggestion and technical support for the field of bioinformatics.

I am deeply grateful to Satoru Nogami, Masashi Yukawa and Keiko Kono for their advice, discussion and encouragement throughout this study.

I wish to thank Emi Shimoi, Yuka Kitamura and Tamao Goto for their technical support in the microscopic observation of the morphological mutants.

I would like to thank Miyuki Imanari, Satomi Oka and Hiroyuki Usuki for their discussion, advice and patient encouragement.

I also thank all the members of the Laboratory of Signal Transduction, Department of Integrated Biosciences, Graduate School of Frontier Sciences, The University of Tokyo, for their warm encouragement and support throughout this study.

Last, but not least, I express my deepest gratitude to my family for their financial support and warm encouragement throughout this study.

TABLE OF CONTENTS

LIST OF FIGURES

LIST OF TABLES

ABBREVIATIONS

CDK	: cyclin-dependent protein kinase
ConA	: concanavalin A
DAPI	: 4',6-diamidino-2-phenylindol
DNA	: deoxyribonucleic acid
EUROSCARF	: European *Saccharomyces cerevisiae* Archive for Functional Analysis
FITC	: fluorescein isothiocyanate
G_1 phase	: gap 1 phase
G_2 phase	: gap 2 phase
GO	: gene ontology
M phase	: mitotic phase
ORF	: open reading frame
PCR	: polymerase chain reaction
Rh-ph	: rhodamine-phalloidin
SD	: synthetic medium supplemented with 2% glucose
SGD	: *Saccharomyces* Genome Database
S phase	: synthetic phase
YPD	: 1% yeast extract, 2% bactopeptone, 2% glucose

ABSTRACT

Cell morphogenesis of *Saccharomyces cerevisiae* is achieved by apical and successive isotropic bud growth. Although the transition from the apical to isotropic bud growth phase is linked to the cell cycle and the actin cytoskeleton is involved in the process, its molecular mechanisms are not fully understood. To obtain a comprehensive view of the budding phase transition, 4,718 yeast haploid non-essential gene deletion mutants were screened with image processing program, *CalMorph*, and 35 mutants with a round bud and 173 mutants with an elongated bud were statistically identified. The functions of the genes whose deletion caused round or elongated bud morphology was divergent, indicating that bud roundness is regulated by plural cellular functions. In these mutants, I found close relationships between bud morphology and cellular functions. The mutants defective in the same components (polarisome, actin cable and actin filament) and in the similar functions (mannosyltransferase activity) are enriched in the round bud mutants. In the elongated bud mutants, similar enrichment was observed. I classified round and elongated bud mutants based on the factors thought to affect the length of apical bud growth phase. I found that two round bud mutants (*arc18* and *sac6*) were defective in apical actin patch localization. In addition, I identified the several elongated bud mutants for which cell cycle-progression delayed at the apical bud growth phase, suggesting that these mutants have defect in control cell cycle-progression.

INTRODUCTION

Apical growth is a growth pattern in which a part of the cell grows in unidirectional. It normally produces the structure of a projection, being indispensable for numerous cellular functions including differentiation, proliferation, and cell morphogenesis of many eukaryotic cells. For example, apical growth is observed during axon outgrowth in neuronal cells and during flower pollen tube elongation at the time of fertilization (Cid-Arregui *et al.*, 1995; Bedinger *et al.*, 1994). Even in a single unicellular organism, the budding yeast *Saccharomyces cerevisiae*, the apical and successive isotropic bud growth phase is required for the formation of normal shape of the bud. In the budding yeast, changes in cell polarity and cell cycle-progression show a close temporal correlation, and this is an unique feature different from the apical growth observed in other organisms (Pruyne and Bretscher, 2000).

The formation of polarized cellular structures is required for the yeast cell morphogenesis. During the vegetative cycle, polarized growth is observed in the bud growth, which is a fundamental process of cell morphogenesis involving dynamic rearrangements of the cytoskeleton (Figure 1, Adams and Pringle, 1984; Lew and Reed, 1993; Pruyne and Bretscher, 2000). Cells first recognize an internal cue that establishes the site of polarization at the cell surface. After selection and establishment of the presumptive bud site in late G_1, polarized growth is achieved by unidirectional transport of secretory vesicles containing newly synthesized membrane components and

cell wall materials along actin cytoskeleton. In the early stage of budding, bud growth is restricted to the distal tip of the growing bud and is termed apical bud growth. Upon entry into mitosis, the cortical actin patches then redistribute throughout the entire bud surface, leading to uniform enlargement of the bud (isotropic bud growth phase). After nuclear division, a repolarization phase begins. During cytokinesis, an actin ring is formed at the mother-bud neck, and new materials are concentrated at the neck. Thus, correct bud shape is formed by a coordination of apical bud growth in the first stage and isotropic bud growth in the second stage of the budding cycle.

The process of selecting and establishing sites of polarized growth has been extensively studied in *S. cerevisiae* (Drubin and Nelson, 1996; Madden and Snyder, 1998). Cell polarity is controlled by the formation of actin cytoskeleton and the cell cycle-progression. First, the actin cytoskeleton is essential for bud growth and is thought to mediate directional transport of secretory vesicles. Both cortical actin patches and components of the secretory apparatus localize to sites of growth. The polarisome complex composed of Spa2p, Pea2p, Bud6p, and Bni1p also participates in yeast morphogenesis (Snyder *et al.*, 1991; Sheu *et al.*, 1998). At the onset of apical bud growth, polarisome complex concentrates at the incipient bud site and remains at the bud tip during the apical bud growth phase. In the absence of polarisome complex, buds appear rounder than wild-type buds (Snyder, 1989; Valtz and Herkowitz, 1996; Amberg *et al.*, 1997; Evangelista *et al.*, 1997).

Second, the timing of the polarity establishment is controlled by the cell cycle

machinery. A previous report indicated that the apical-isotropic switch is regulated through activation of Cdc28p, a major cyclin-dependent kinase (CDK) of the budding yeast (Lew and Reed, 1993). Activation of Cdc28p by G_1 cyclins, Cln1p and Cln2p, triggers bud emergence and apical bud growth, while activation of Cdc28p by the mitotic cyclins, Clb1p and Clb2p, causes bud growth to isotropic. Inactivation of Clb-dependent Cdc28p kinase results in termination of the isotropic bud growth phase, inducing cytokinesis (Lew and Reed, 1995). Consistent with this theory, elongated bud morphology was induced by the extended apical bud growth phase caused by a specific *cdc28* mutation (*cdc28*^{ECP}) defective in the G_2/M transition (Ahn *et al.*, 2001), by constitutive expression of G_1 cyclins (Loeb *et al.*, 1999), or by deletion of a major G_2 cyclin gene, *CLB2* (Ahn *et al.*, 1999). In addition, a *cdc34-2* mutant also showed prolonged apical growth phase, eventually forming multiple highly elongated buds (Goebl *et al.*, 1988). This mutant carrying a temperature sensitive allele of *CDC34*, a yeast E2 ubiquitin-conjugating enzyme gene, fail to degrade the G_1 cyclins (Deshaies *et al.*, 1995; Yaglom *et al.*, 1995), and the G_2 cyclin/CDK inhibitor, Sic1p (Schwob *et al.*, 1994; Mendenhall and Hodge, 1998) at the restrictive temperature. Thus, it is expected that the bud shape also become abnormal by mutation of the gene that regulates cell cycle-progression. Bud initiation occurs in late G_1, and cell polarity alteration correlate with cell cycle-progression (Lew and Reed, 1995), but little is known of how timing is controlled.

In order to have a comprehensive view of the apical bud growth control, I

think systematic genome-wide morphological screening is the most fruitful, because a large number of molecules are considered to be involved in this process. Although several morphological screens were performed in the budding yeast aiming to identify the factors involved in apical bud growth control (Blacketer *et al.*, 1995; Mosch and Fink, 1997; Bidlingmaier and Snyder, 2002), they lack a comprehensive and quantitative viewpoint. In *Saccharomyces cerevisiae*, whole genome sequences were determined in 1996 (Goffeau *et al.*, 1996), and we can use a set of the strains containing systematic deletions of yeast ORFs generated by *Saccharomyces* Genome Deletion Project (Winzeler *et al.*, 1999). Despite rapidly accumulating information, all tasks in morphological researches have been performed manually: observation of a series of mutant cells under microscope and qualitative classification by comparison visually (Giaever *et al.*, 2002).

Our laboratory developed a novel system for automatic image processing that enabled us to gather efficiently reproducible and quantitative morphological data from a massive amount of fluorescent micrographs (Figure 2, Ohtani *et al.*, 2004; Saito *et al.*, 2004). Using this system, 4,718 haploid non-essential gene deletion mutants were analyzed (Ohya *et al.*, 2005). In this study, 2,378 of 4,718 mutants have significant changes in at least one of the morphological parameters. It was also shown that there are close relationship between morphology and a function of the gene product. Analysis of mutant morphological phenotype is effective methods for attributing functions to genes.

In this study, I identified the mutants with abnormal bud morphology using quantitative morphological data. Based on massive amount of morphological parameters, I classified these mutants. I found that actin cytoskeleton defect may cause loss of polarized secretion and leads round bud phenotype. I also found that mutants defective in cell cycle-progression showed abnormal bud morphology.

RESULTS AND DISCUSSION

Identification of gene deletion mutants with abnormal bud morphology

In the budding yeast *Saccharomyces cerevisiae*, apical bud growth is usually observed at the period between bud emergence and nuclear division. Therefore, in order to screen mutants defective in apical bud growth control, I focused on the cells with a single nucleus at the cell cycle stage before nuclear division. The degree of bud elongation at this stage is expressed as a value of a morphological parameter, C114_A1B (bud axis ratio of budded cells with a single nucleus), defined as the ratio of the growth axis length of the bud (axis A) and the axis length perpendicularly crossing the axis A (axis B) of budded cells with a single nucleus (Figure 3A). Among total of 4,718 haploid non-essential gene deletion mutants, 35 and 173 yeast mutants were statistically identified ($P < 0.0001$) as round and elongated bud mutants, respectively (Figure 3B and Table 1). This threshold value was decided for the false-positive mutant to become less than one at the examination of 4,718 mutants. Besides C114_A1B, there are two other related parameters, mother axis ratio of budded cells with a single nucleus (C115_A1B) and bud axis ratio of budded cells with two nuclei (C114_C) (Figure 3A). I noticed that 75 % and 83 % of the mutants identified by C114_A1B were overlapped with the ones identified by C115_A1B and C114_C, respectively (Figure 3CD). The distribution of 126 independently collected wild-type values of C114_A1B was wider than that of C115_A1B or C114_C. This suggests that

C114_A1B well reflects heterogeneous bud axis ratio of cells during apical bud growth.

Several gene modules specified by GO affect bud axis ratio

I found close relationship between bud roundness of the mutants and cellular functions using Gene Ontology (GO). The GO project was established to provide a common language to describe aspects of a gene product's biology (Ashburner *et al.*, 2000; Dwight *et al.*, 2002). The use of a consistent vocabulary allows genes from different species to be compared based on their GO annotations. The objective of GO is to provide controlled vocabularies for the description of the molecular function, biological process and cellular component of gene products. First, 'GO slim mapper' was used to investigate relationship between morphology and cellular functions. This tool determines to which GO terms a set of yeast genes is annotated. In 35 genes whose deletion caused a round bud, GO terms 'organelle organization and biogenesis,' 'transport' and 'cytoskeleton organization and biogenesis' were frequently annotated (14, 10, and 11 genes, respectively). In 173 genes whose deletion caused an elongated bud, GO terms 'organelle organization and biogenesis,' 'DNA metabolism' and 'transport and protein modification' were frequently found (52, 37, and 26 genes, respectively). Six of round bud mutants and 28 of elongated bud mutants carried a deletion in a gene of unknown function. It is difficult to reveal which cellular functions relate to bud roundness by this analysis because the same gene were annotated in different GO terms, and the listed GO terms did not represent specific functions.

However, these results indicate that several genes in particular GO terms have relationship to roundness of bud, suggesting that the roundness of bud is regulated by plural cellular functions.

Then, I looked for GO terms where genes whose deletion causes abnormal bud morphology were significantly enriched. For example, polarisome is a protein complex that helps determination of cell polarity (Pruyne and Bretscher, 2000), and therefore, four of five polarisome mutants (annotated by GO consortium) harbored round bud phenotype. In the round bud mutants, the enrichment of polarisome mutants occurred by chance with a probability of 1.14×10^{-8} (binomial test, Figure 4), indicating that a round bud is a characteristic feature caused by loss of the polarisome function. By using 'GO term Finder,' I obtained a global view of the correlation. Four GO terms for the round bud mutants and 11 for the elongated bud mutants were identified (Table 2).

In the round bud mutants, mutants deleted with the same components ('polarisome,' 'actin cable' and 'actin filament') were enriched. Polarisome complex, including Spa2p, Bni1p, Bud6p and Pea2p, localizes to sites of polarized growth, and is involved in the dynamic organization of the actin cytoskeleton during polarized growth (Sheu *et al.*, 1998). The localization of Spa2p to sites of polarized growth depends on Myo2p. Spa2p, like Myo2p, cosediments with F-actin in a ATP-sensitive manner (Shih *et al.*, 2005). Bni1p containing the FH1FH2 domains increases the rate of filament nucleation from pure G-actin (Pruyne *et al.*, 2002). *TPM1* encodes the major

isoform of yeast tropomyosin. Tpm1p localize specifically to actin cables and not cortical patches. Actin cables are highly unstable in the absence of tropomyosin and are rapidly restored in its presence (Pruyne *et al.*, 1998). Myo2p-dependent polarized delivery of secretory vesicles requires actin cables (Pruyne *et al.*, 1998). Therefore, actin cytoskeleton defect may cause loss of polarized secretion and leads round bud phenotype in these mutants.

Mutants deleted with the similar functions ('mannosyltransferase activity') were enriched in the round bud mutants. Och1p is responsible for addition of the first mannose residue to the core oligosaccharides obtained in the ER (Nakayama *et al.*, 1992). Because mannan constitutes one of the major cell wall components of yeast as mannoproteins, the defect in cell wall organization in *och1* cells may cause round bud phenotype.

Several deletion mutants of the genes annotated to the same GO term showed no phenotypic alteration (shown in black). For example, although the *SPH1* gene annotated to the GO term 'polarisome,' the *sph1* mutant showed normal bud morphology. This is consistent with the previous report suggesting Sph1p specifically functions at the polarized growth of mating projection rather than normal budding (Roemer *et al.*, 1998), although Sph1p is related both structurally and functionally to Spa2p. *TPM2* encodes a minor isoform of tropomyosin. It is known that disruption of *TPM2* alone shows no phenotype (Drees *et al.*, 1995). The *HOC1* gene encodes a putative glycosyltransferase similar to Och1p. However, *hoc1* display no detectable

defect in protein glycosylation, and *HOC1* overexpression cannot rescue *och1*, suggesting that Hoc1p have a distinct role from Och1p (Neiman *et al.*, 1997). Although *cap2*, *mnn10*, and *mnn11* mutant showed no significant difference, their values were near to threshold. Therefore, it is thought that these results are consistent with previous studies.

In the elongated bud mutants, mutants deleted with the same cellular processes ('response to phosphate starvation,' 'proline biosynthesis' and 'septin checkpoint'), with the similar functions ('ribonucleoside-diphosphate reductase' and 'rDNA binding'), and with the same complexes ('SWR1,' 'SLIK,' 'Ada2/Gcn5/Ada3 transcription activator,' 'Cdc73/Paf1,' 'RNA polymerase I transcription factor' and 'chromatin assembly') were enriched (Table 2). In these groups, septin checkpoint is especially interesting. Septins are present in eukaryotes ranging from yeast to mammals, and have a conserved role in cytokinesis and/or cell septation (Longtine *et al.*, 1996). In the budding yeast, it is known that septins function in many other processes, including the selection of the bud site chitin deposition, spindle orientation, and cell cycle-progression (Faty *et al.*, 2002). Correct formation of a functional septin cytoskeleton permits the cell to switch from apical to isotropic bud growth and the onset of mitotic chromosome segregation. Septin defects are detected by septin checkpoint, a cell cycle checkpoint that responds by inhibiting the mitotic CDK. In the presence of septin defects, the mitotic CDK is inactivated and both the switch to isotropic bud growth and the onset of mitotic chromosome segregation is delayed (Barral *et al.*, 1999).

Therefore, it suggests that Clb-CDK activity is inhibited in the septin mutants and cells harbor elongated bud morphology. Relationship between bud morphology and Clb-CDK activity are further discussed in a later section.

Analysis of round bud mutants using quantitative statistic data

It was shown that there are close relationship between morphology and a function of the gene product (Ohya *et al.*, 2005). In addition to roundness of bud, polarisome mutants (*bni1*, *bud6*, *spa2* and *pea2*) exhibited abnormal morphologies in other seven morphological parameters. Therefore, loss of specific cellular functions may simultaneously result in various morphological abnormalities. This allows me to study correlation of the mutant values among the several parameters. In cells during apical bud growth, cortical actin patch clusters at the bud tip (Pruyne and Bretscher, 2000). Thus, I focused on the percentage of cells with cortical actin patch localized only at the bud tip (apical actin). In Figure 5, a correlation of round bud mutants is investigated between bud axis ratio of budded cells with a single nucleus (C114_A1B) and apical actin ratio in budded cells (A116). I found that two round bud mutants (*arc18* and *sac6*) exhibited significantly lower values ($P < 0.0001$) in both C114_A1B and A116. Arc18p and Sac6p are known to be involved in control of the spatial distribution of actin filaments (Winter *et al.*, 1999; Karpova *et al.*, 1995). Short apical growth phase may cause round bud morphology in these mutants.

To confirm this, individual cell morphologies of each mutant cell ($n > 200$)

are examined. Figure 7 represents the landmark events during the cell cycle, including their bud morphology, actin localization, and number and position of nucleus. In Figure 7, the horizontal axis is displayed in the rank order of ratio of bud size to mother cell size of individual cell and normalized to become the same width. This axis is thought to reflect bud growth. The vertical axis is displayed bud axis ratio with a single nucleus (C114_A1B). The dots are colorized with the state of nucleus and actin localization. The plot of the wild-type cells indicates that the buds unidirectionally grew immediately after bud emergence (apical bud growth phase), judged from the steep slope of the graph. After that, buds obtained both length and width (isotropic bud growth phase), judged from the constant bud axis ratio. The average of the bud axis ratio of *arc18* and *sac6* was smaller than the wild-type indicating that the bud of these mutants are rounder than that of wild-type. These mutant cells harbored very few polarized actin after bud emergence supporting the idea that the loss of apical actin distribution causes inability to elongate a bud in *arc18* and *sac6* mutant cells.

Apical bud growth is mainly observed in the small-budded cells before nuclear division (Figure 7, Tjandra *et al.*, 1998; Rua *et al.*, 2001). In Figure 6, a correlation of round bud mutants is investigated between bud axis ratio (C114_A1B) and single nucleus ratio in budded cells (D207). I found that 3 round bud mutants (*cog1*, *och1* and *arc18*) exhibited significantly lower values ($P < 0.0001$) in D207. Figure 7 shows that ratio of cells before nuclear division decreased in these mutants, suggesting that the shorter period before nuclear division cause round shape of bud.

Classification of elongated bud mutants by actin localization

Next, elongated bud mutants were classified by using quantitative statistic data. I examined actin localization at each phase of cell cycle. In Figure 8, values of A107_A1B (apical actin ratio of budded cells with a single nucleus) and A107_C (apical actin ratio of budded cells with two nuclei) of elongated bud mutants are plotted in a horizontal axis and vertical axis, respectively. I found 3 groups that showed the different distribution from 126 replicates of wild-type measurement: (1) 5 elongated bud mutants (*arp8*, *akr1*, *arp5*, *tps1* and *ies6*) exhibited higher values of apical actin ratio throughout the cell cycle, (2) 2 elongated bud mutants (*rrn10* and *paf1*) exhibited higher values only after nuclear division, (3) 4 elongated bud mutants (*ykl121w*, *bud13*, *ylr407w* and *swc3*) exhibited higher values only before nuclear division (Figure 8). In these mutants, distinct apical bud growth phase might cause each elongated bud phenotype. To further investigate these phenotypes, individual cell morphologies of typical mutants are shown in Figure 9. In the group (1), the values of bud axis ratio continued to increase to the end of the cell cycle. This result suggests that the timing of the apical-isotropic switch is retarded or defective in these mutants. Contrary, in the group (3), the apical bud growth of small-budded cells was extremely extended, and the obvious isotropic bud growth phase in medium/large-budded cells was found. It was shown that the bud morphology of living cells overexpressing *CLN2* became highly elongated before the nuclear division (Loeb *et al.*, 1999). The enhancement of the

apical bud growth observed in the group (3) might be related to the expression of G_1 cyclins.

Classification of elongated bud mutants by state of nucleus

It is expected that the longer the period from bud emergence to nuclear division extend, the longer the apical bud growth phase extend. In Figure 10, a correlation between C114_A1B (bud axis ratio of cells with a single nucleus) and D207 (single nucleus ratio in budded cells) of elongated bud mutants is investigated. I found that 5 mutants (*clb2*, *rnr4*, *pet130*, *yke2* and *ylr407w*) exhibited significantly higher values ($P < 0.0001$) in D207. To further examine this phenotype, individual cell morphologies are examined (Figure 11). I found that the phase before nuclear division of these mutants is longer than wild-type. This group classified by D207 contained *clb2* mutant, and showed the defect of cell cycle-dependent bud morphogenesis and nuclear division. In G_2 phase, mitotic cyclins Clb1p/Clb2p-CDK activation triggers the apical-isotropic switch (Lew and Reed, 1993). Clb2p plays a major role in promoting M-phase, despite its functional redundancy with three closely related cyclins Clb1p, Clb3p and Clb4p. This result suggests that cell cycle-progression is delayed in these mutants and these genes might be involved in the regulation of Clb2p expression or the activity of Clb2p-CDK.

In this study, I found several cellular functions that correlate with bud roundness. Focused on the actin localization, I found mutants that showed actin cytoskeleton defect.

Focused on the length of period from bud emergence to nuclear division, I found mutants that showed the defect of cell cycle-progression. To obtain new finding concerning timing control of polarized cell growth, I will try to examine the amount of cyclins in these mutants in the future.

MATERIALS AND METHODS

Strains, Media, Growth conditions and Genetic manipulations

A set of haploid *Saccharomyces cerevisiae MAT***a** deletion strains (4,718 strains) was obtained from the European *Saccharomyces cerevisiae* Archive for Functional Analysis (EUROSCARF). These strains are congenic derivatives of BY4741, which is itself a descendant of S288C (Brachmann *et al.*, 1998). Most of the strains contain precise deletions in which the entire ORF after the ATG is replaced with a *kanMX4* marker (Winzeler *et al.*, 1999).

Yeast cells were grown either in rich medium [YPD; 1% Bacto-yeast extract (Difco), 2% Bacto-peptone (Difco), 2% glucose (Wako Chemicals, Osaka, Japan)] or in synthetic growth medium [SD; 0.67% yeast nitrogen base without amino acid (Difco), 2% glucose], with appropriate supplements. The final concentration of each amino acid is 20 μg/ml for adenine, uracil, triptophan, histidine and methionine, and 30 μg/ml for leucine and lysine. Solid media contained 2% agar (Shouei Chemicals, Tokyo, Japan).

Yeast strains were cultured at 25℃. Standard procedures were used for the DNA manipulations (Sambrook *et al.*, 1989). Crossing, sporulation and tetrad analysis were performed as described previously (Rose *et al.*, 1989).

Image processing with CalMorph

Image processing with *CalMorph* (ver. 1.0) software was performed as described previously (Ohtani *et al.*, 2004). To obtain fluorescent images of morphology of all yeast mutants, log-phase yeast cells were fixed with formaldehyde and then stained with rhodamine-phalloidin (for actin), FITC-ConA (for the cell wall), and DAPI (for the nucleus). Images were captured using the Zeiss Axioplan 2CCD camera (Cool SNAP HQ; Roper Scientific) and the Metamorph Imaging software (Universal Imaging). Captured images were processed with the *CalMorph* software. The obtained images of all yeast mutants and data-mining functions are available at *Saccharomyces cerevisiae* Morphological Database (SCMD) web site (http://scmd.gi.k.u-tokyo.ac.jp).

Judging morphological mutants

Statistical tests are not applicable to this data set because we have only one set of data for each deletion strain. Thus, we defined morphological normality of a deletion strain as the probability that data from wild-type cells would have measurements outside the range of the deletion strains. The measurement of morphological abnormality was described in Ohya *et al.* (2005).

Gene Ontology (GO) analysis

The GO-gene associations used in this study were published in the *Saccharomyces* genome database (SGD) at Aug. 31, 2005. 'GO slim mapper' is available at

http://db.yeastgenome.org/cgi-bin/GO/goTermMapper, 'GO term Finder' at http://db.yeastgenome.org/cgi-bin/GO/goTermFinder.

Verification of mutant strains

Disruption of the corresponding genes by replacement kanamycin-resistant gene cassette was verified by PCR for some mutants with abnormal bud. Primer kanB, CTGCAGCGAGGAGCCGTAAT, and primer of each mutant strain generate about 0.8 kb PCR product from genomic DNA of each mutant cell. For amplification of genomic DNA by PCR, *TaKaRa Ex Taq*^{tm} (TaKaRa Biochemicals, Shiga, Japan). Primers used in this manipulation are listed in Table 4.

REFERENCES

Adams A.E., Pringle J.R. (1984)
Relationship of actin and tubulin distribution to bud growth in wild-type and morphogenetic-mutant *Saccharomyces cerevisiae*. *J. Cell Biol.* **98**, 934-45.

Ahn S.H., Acurio A., Kron S.J. (1999)
Regulation of G_2/M progression by the STE mitogen-activated protein kinase pathway in budding yeast filamentous growth. *Mol. Biol. Cell* **10**, 3301-16.

Ahn S.H., Tobe B.T., Fitz Gerald J.N., Anderson S.L., Acurio A., Kron S.J. (2001)
Enhanced cell polarity in mutants of the budding yeast cyclin-dependent kinase Cdc28p. *Mol. Biol. Cell* **12**, 3589-600.

Amberg D.C., Zahner J.E., Mulholland J.W., Pringle J.R., Botstein D. (1997)
Aip3p/Bud6p, a yeast actin-interacting protein that is involved in morphogenesis and the selection of bipolar budding sites. *Mol. Biol. Cell* **8**, 729-53.

Ashburner M., Ball C.A., Blake J.A., Botstein D., Butler H., Cherry J.M., Davis A.P., Dolinski K., Dwight S.S., Eppig J.T., Harris M.A., Hill D.P., Issel-Tarver L., Kasarskis A., Lewis S., Matese J.C., Richardson J.E., Ringwald M., Rubin G.M., Sherlock G. (2000)
Gene ontology: tool for the unification of biology. The Gene Ontology Consortium. *Nat. Genet.* **25**, 25-9.

Barral Y., Parra M., Bidlingmaier S., Snyder M. (1999)
Nim1-related kinases coordinate cell cycle progression with the organization of the peripheral cytoskeleton in yeast. *Genes Dev.* **13**, 176-87.

Bedinger P.A., Hardeman K.J., Loukides C.A. (1994)
Travelling in style: the cell biology of pollen. *Trends Cell Biol.* **4**, 132-8.

Bidlingmaier S., Snyder M. (2002)
Large-scale identification of genes important for apical growth in *Saccharomyces cerevisiae* by directed allele replacement technology (DART) screening. *Funct. Integr. Genomics* **1**, 345-56.

Blacketer M.J., Madaule P., Myers A.M. (1995)
Mutational analysis of morphologic differentiation in *Saccharomyces cerevisiae*. *Genetics* **140**, 1259-75.

Brachmann C.B., Davies A., Cost G.J., Caputo E., Li J., Hieter P., Boeke J.D. (1998)
Designer deletion strains derived from *Saccharomyces cerevisiae* S288C: a useful set of strains and plasmids for PCR-mediated gene disruption and other applications. *Yeast* **14**, 115-32.

Cid-Arregui A., De Hoop M., Dotti C.G. (1995)
Mechanisms of neuronal polarity. *Neurobiol. Aging* **16**, 239-46.

Deshaies R.J., Chau V., Kirschner M. (1995)
Ubiquitination of the G_1 cyclin Cln2p by a Cdc34p-dependent pathway. *EMBO J.* **14**, 303-12.

Drees B., Brown C., Barrell B.G., Bretscher A. (1995)
Tropomyosin is essential in yeast, yet the *TPM1* and *TPM2* products perform distinct functions. *J. Cell Biol.* **128**, 383-92.

Drubin D.G., Nelson W.J. (1996)
Origins of cell polarity. *Cell* **84**, 335-44.

Dwight S.S., Harris M.A., Dolinski K., Ball C.A., Binkley G., Christie K.R., Fisk D.G., Issel-Tarver L., Schroeder M., Sherlock G., Sethuraman A., Weng S., Botstein D., Cherry J.M. (2002)

Saccharomyces Genome Database (SGD) provides secondary gene annotation using the Gene Ontology (GO). *Nucleic Acids Res.* **30**, 69-72.

Evangelista M., Blundell K., Longtine M.S., Chow C.J., Adames N., Pringle J.R., Peter M., Boone C. (1997)
Bni1p, a yeast formin linking Cdc42p and the actin cytoskeleton during polarized morphogenesis. *Science* **276**, 118-22.

Faty M., Fink M., Barral Y. (2002)
Septins: a ring to part mother and daughter. *Curr. Genet.* **41**, 123-31.

Giaever G., Chu A.M., Ni L., Connelly C., Riles L., Veronneau S., Dow S., Lucau-Danila A., Anderson K., Andre B., Arkin A.P., Astromoff A., El-Bakkoury M., Bangham R., Benito R., Brachat S., Campanaro S., Curtiss M., Davis K., Deutschbauer A., Entian K.D., Flaherty P., Foury F., Garfinkel D.J., Gerstein M., Gotte D., Guldener U., Hegemann J.H., Hempel S., Herman Z., Jaramillo D.F., Kelly D.E., Kelly S.L., Kotter P., LaBonte D., Lamb D.C., Lan N., Liang H., Liao H., Liu L., Luo C., Lussier M., Mao R., Menard P., Ooi S.L., Revuelta J.L., Roberts C.J., Rose M., Ross-Macdonald P., Scherens B., Schimmack G., Shafer B., Shoemaker D.D., Sookhai-Mahadeo S., Storms R.K., Strathern J.N., Valle G., Voet M., Volckaert G., Wang C.Y., Ward T.R., Wilhelmy J., Winzeler E.A., Yang Y., Yen G., Youngman E., Yu K., Bussey H., Boeke J.D., Snyder M., Philippsen P., Davis R.W., Johnston M. (2002)
Functional profiling of the *Saccharomyces cerevisiae* genome. *Nature* **418**, 387-91.

Goebl M.G., Yochem J., Jentsch S., McGrath J.P., Varshavsky A., Byers B. (1988)
The yeast cell cycle gene *CDC34* encodes a ubiquitin-conjugating enzyme. *Science* **241**, 1331-5.

Goffeau A., Barrell B.G., Bussey H., Davis R.W., Dujon B., Feldmann H., Galibert F., Hoheisel J.D., Jacq C., Johnston M., Louis E.J., Mewes H.W., Murakami Y., Philippsen P., Tettelin H., Oliver S.G. (1996)

Life with 6000 genes. *Science* **274**, 546, 563-7.

Karpova T.S., Tatchell K., Cooper J.A. (1995)
Actin filaments in yeast are unstable in the absence of capping protein or fimbrin. *J. Cell Biol.* **131**, 1483-93.

Lew D.J., Reed S.I. (1993)
Morphogenesis in the yeast cell cycle: regulation by Cdc28 and cyclins. *J Cell Biol.* **120**, 1305-20.

Lew D.J., Reed S.I. (1995)
Cell cycle control of morphogenesis in budding yeast. *Curr. Opin. Genet. Dev.* **5**,17-23.

Loeb J.D., Kerentseva T.A., Pan T., Sepulveda-Becerra M., Liu H. (1999)
Saccharomyces cerevisiae G_1 cyclins are differentially involved in invasive and pseudohyphal growth independent of the filamentation mitogen-activated protein kinase pathway. *Genetics* **153**, 1535-46.

Longtine M.S., Fares H., Pringle J.R. (1998)
Role of the yeast Gin4p protein kinase in septin assembly and the relationship between septin assembly and septin function. *J. Cell Biol.* **143**, 719-36.

Madden K., Snyder M. (1998)
Cell polarity and morphogenesis in budding yeast. *Annu. Rev. Microbiol.* **52**, 687-744.

Mendenhall M.D., Hodge A.E. (1998)
Regulation of Cdc28 cyclin-dependent protein kinase activity during the cell cycle of the yeast *Saccharomyces cerevisiae*. *Microbiol Mol. Biol. Rev.* **62**, 1191-243.

Mosch H.U., Fink G.R. (1997)
Dissection of filamentous growth by transposon mutagenesis in *Saccharomyces cerevisiae*. *Genetics* **145**, 671-84.

Nakayama K., Nagasu T., Shimma Y., Kuromitsu J., Jigami Y. (1992)
OCH1 encodes a novel membrane bound mannosyltransferase: outer chain elongation of asparagine-linked oligosaccharides. *EMBO J.* **11**, 2511-9.

Neiman A.M., Mhaiskar V., Manus V., Galibert F., Dean N. (1997)
Saccharomyces cerevisiae HOC1, a suppressor of pkc1, encodes a putative glycosyltransferase. *Genetics* **145**, 637-45.

Ohtani M., Saka A., Sano F., Ohya Y., Morishita S. (2004)
Development of image processing program for yeast cell morphology. *J. Bioinform. Comput. Biol.* **1**, 695-709.

Ohya Y., Sese J., Yukawa M., Sano F., Nakatani Y., Saito T.L., Saka A., Fukuda T., Ishihara S., Oka S., Suzuki G., Watanabe M., Hirata A., Ohtani M., Sawai H., Fraysse N., Latge J.P., Francois J.M., Aebi M., Tanaka S., Muramatsu S., Araki H., Sonoike K., Nogami S., Morishita S. (2005)
High-dimensional and large-scale phenotyping of yeast mutants. *Proc. Nat. Acad. Sci. U S A* **102**, 19015-20.

Pruyne D.W., Schott D.H., Bretscher A. (1998)
Tropomyosin-containing actin cables direct the Myo2p-dependent polarized delivery of secretory vesicles in budding yeast. *J. Cell Biol.* **143**, 1931-45.

Pruyne D., Bretscher A. (2000)
Polarization of cell growth in yeast. I. Establishment and maintenance of polarity states. *J. Cell Sci.* **113**, 365-75.

Pruyne D., Bretscher A. (2000)
Polarization of cell growth in yeast. II. The role of the cortical actin cytoskeleton. *J. Cell Sci.* **113**, 571-585.

Pruyne D., Evangelista M., Yang C., Bi E., Zigmond S., Bretscher A., Boone C. (2002)
Role of formins in actin assembly: nucleation and barbed-end association. *Science* **297**, 612-5.

Roemer T., Vallier L., Sheu Y.J., Snyder M. (1998)
The Spa2-related protein, Sph1p, is important for polarized growth in yeast. *J. Cell Sci.* **111**, 479-94.

Rose M.D., Winston F., Hieter P. (1990)
Laboratory course manual for methods in yeast genetics. *Cold Spring Harbor Laboratory Press*

Rua D., Tobe B.T., Kron S.J. (2001)
Cell cycle control of yeast filamentous growth. *Curr Opin Microbiol.* **4**, 720-7.

Saito T.L., Ohtani M., Sawai H., Sano F., Saka A., Watanabe D., Yukawa M., Ohya Y., Morishita S. (2004)
SCMD: *Saccharomyces cerevisiae* Morphological Database. *Nucleic Acids Res.* **32**, D319-22.

Sambrook J., Fritsch E.F., Maniatis T. (1989)
Molecular cloning: A laboratory manual/second edition. *Cold Spring Harbor Laboratory Press*

Schwob E., Bohm T., Mendenhall M.D., Nasmyth K. (1994)
The B-type cyclin kinase inhibitor p40SIC1 controls the G_1 to S transition in *S. cerevisiae*. *Cell* **79**, 233-44.

Sheu Y.J., Santos B., Fortin N., Costigan C., Snyder M. (1998)
Spa2p interacts with cell polarity proteins and signaling components involved in yeast cell morphogenesis. *Mol. Cell Biol.* **18**, 4053-69.

Shih J.L., Reck-Peterson S.L., Newitt R., Mooseker M.S., Aebersold R., Herskowitz I. (2005)
Cell polarity protein Spa2p associates with proteins involved in actin function in *Saccharomyces cerevisiae*. *Mol. Biol. Cell* **16**, 4595-608.

Snyder M. (1989)
The SPA2 protein of yeast localizes to sites of cell growth. *J. Cell Biol.* **108**, 1419-29.

Snyder M., Gehrung S., Page B.D. (1991)
Studies concerning the temporal and genetic control of cell polarity in *Saccharomyces cerevisiae*. *J. Cell Biol.* **114**, 515-32.

Tjandra H., Compton J., Kellogg D. (1998)
Control of mitotic events by the Cdc42 GTPase, the Clb2 cyclin and a member of the PAK kinase family. *Curr. Biol.* **8**, 991-1000.

Valtz N., Herskowitz I. (1996)
Pea2 protein of yeast is localized to sites of polarized growth and is required for efficient mating and bipolar budding. *J. Cell Biol.* **135**, 725-39.

Winter D.C., Choe E.Y., Li R. (1999)
Genetic dissection of the budding yeast Arp2/3 complex: a comparison of the in vivo and structural roles of individual subunits. *Proc. Natl. Acad. Sci. U S A* **96**, 7288-93.

Winzeler E.A., Shoemaker D.D., Astromoff A., Liang H., Anderson K., Andre B., Bangham R., Benito R., Boeke J.D., Bussey H., Chu A.M., Connelly C., Davis K., Dietrich F., Dow S.W., El Bakkoury M., Foury F., Friend S.H., Gentalen E., Giaever G., Hegemann J.H., Jones T., Laub M., Liao H., Liebundguth N., Lockhart D.J., Lucau-Danila A., Lussier M., M'Rabet N., Menard P., Mittmann M., Pai C., Rebischung C., Revuelta J.L., Riles L., Roberts C.J., Ross-MacDonald P., Scherens B., Snyder M., Sookhai-Mahadeo S., Storms R.K., Veronneau S., Voet M., Volckaert G., Ward T.R., Wysocki R., Yen G.S., Yu K., Zimmermann K., Philippsen P., Johnston M., Davis R.W.

(1999)
Functional characterization of the *S. cerevisiae* genome by gene deletion and parallel analysis. *Science* **285**, 901-6.

Yaglom J., Linskens M.H., Sadis S., Rubin D.M., Futcher B., Finley D. (1995)
p34Cdc28-mediated control of Cln3 cyclin degradation. *Mol. Cell Biol.* **15**, 731-41.

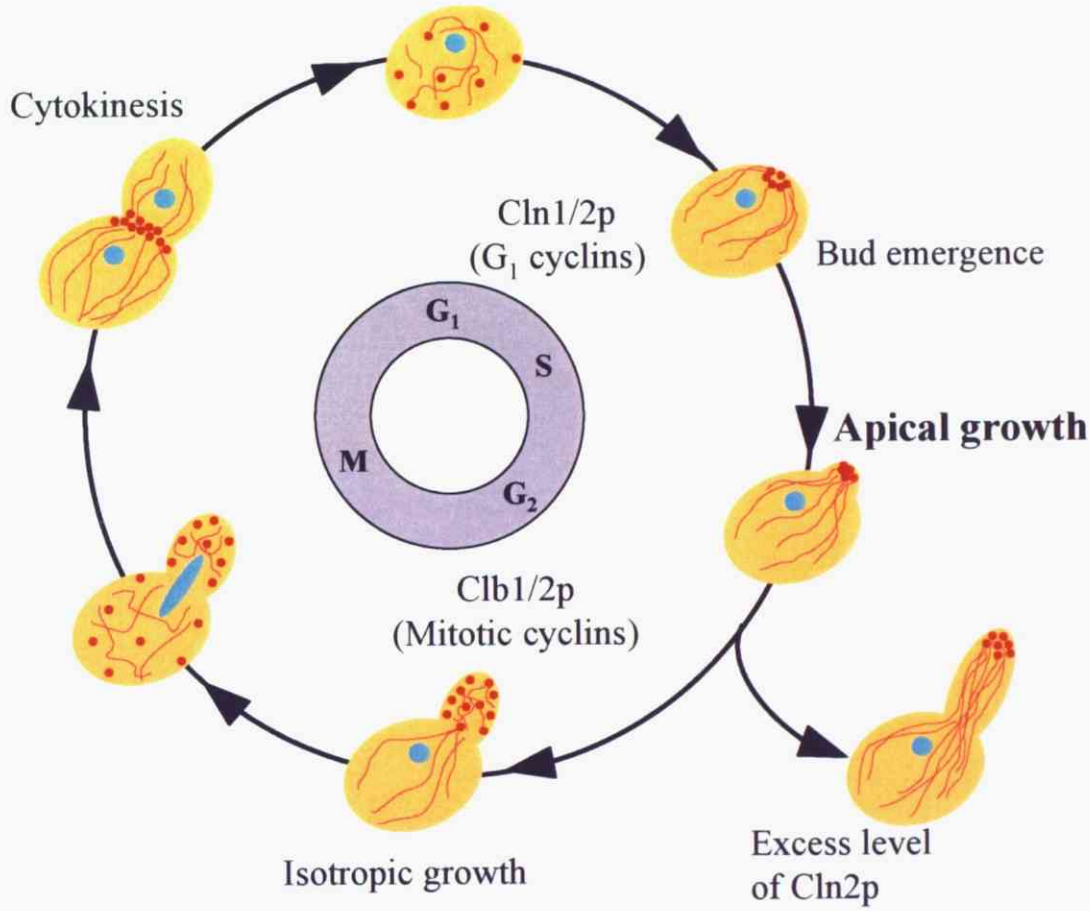

Figure 1. Cell cycle-dependent polarized growth in the budding yeast.
Cell cycle-dependent actin distribution and the cell cycle-progression are described. In G_1 phase, actin patches are delocalized to the cell periphery, then actin patches are polarized to the bud site in G_1/S phase. Apical growth is specifically observed immediately after the bud emergence. The daughter cell grows isotropically in the majority of the bud morphogenetic process. In late-M to cytokinesis, actin rings are assembled at the bud necks, and then a cell is separated into two. Overexpression of G_1 cyclins leads to irregular bud elongation. G_1 and mitotic cyclins are activated at the indicated phase.

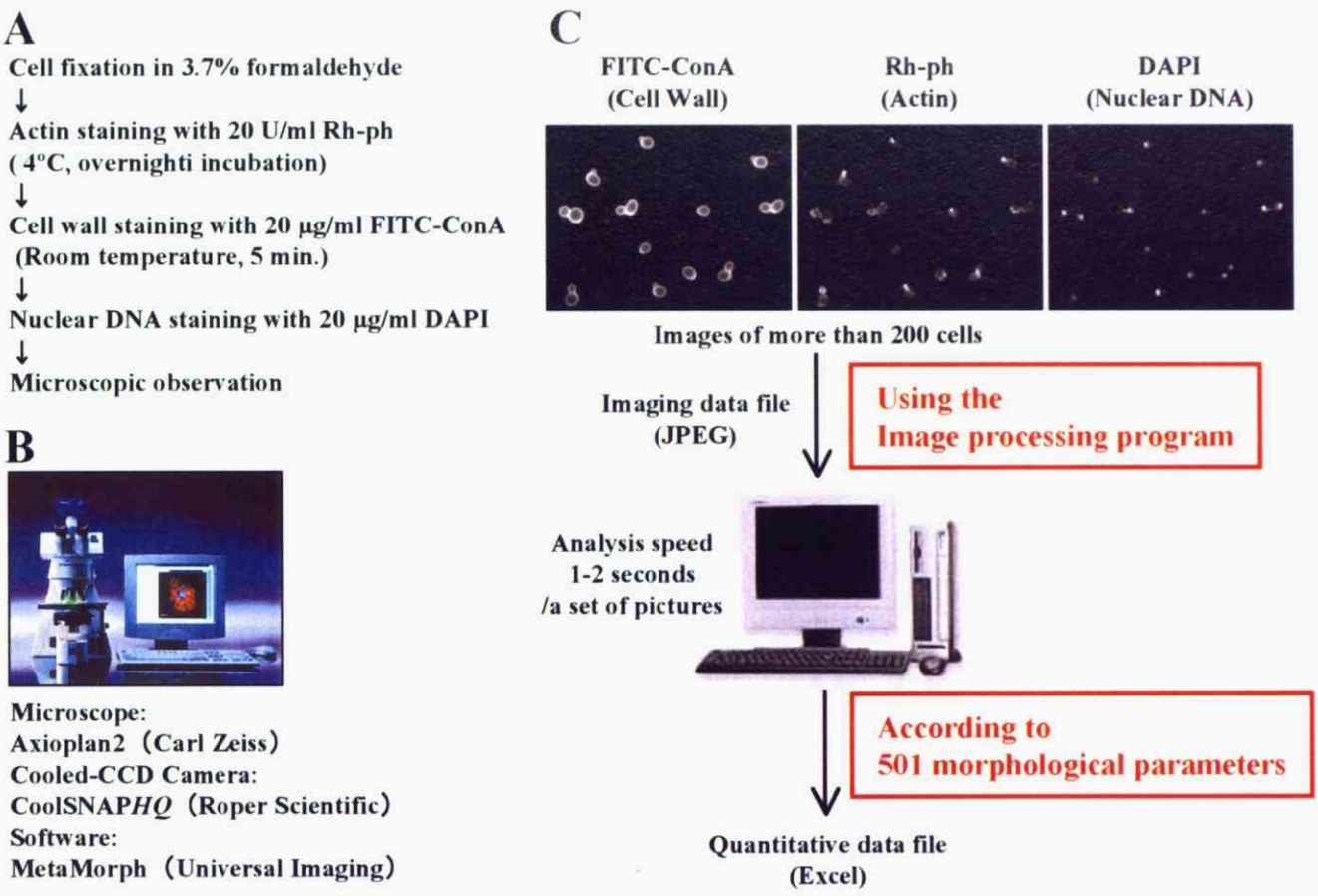

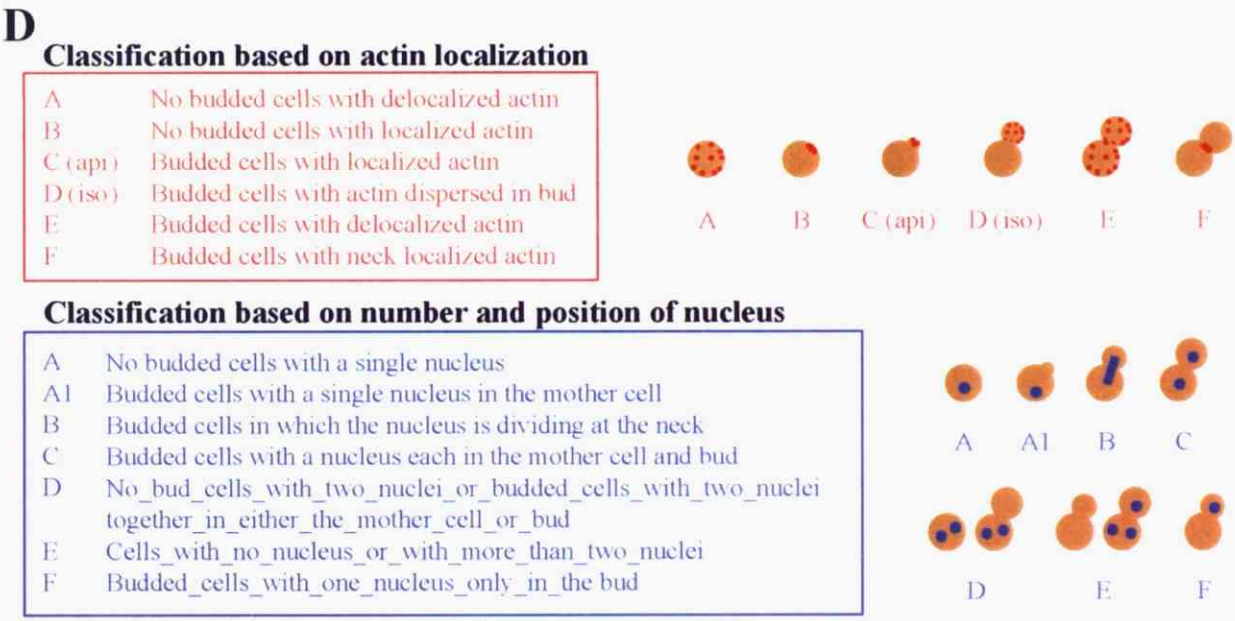

Figure 2. Scheme of the image processing for the budding yeast.
(A) The protocol of triple staining of yeast cells. (B) The environment for taking micrographs. (C) Three images are obtained from one field of view, and data of more than 200 cells are collected. After cell images are saved in JPEG format, an image processing program, *CalMorph* enables us to obtain cell morphology data in EXCEL format within 1-2 seconds per a set of pictures. (D) Definition of the groups. Each cell is classified by actin localization and number and position of nucleus.

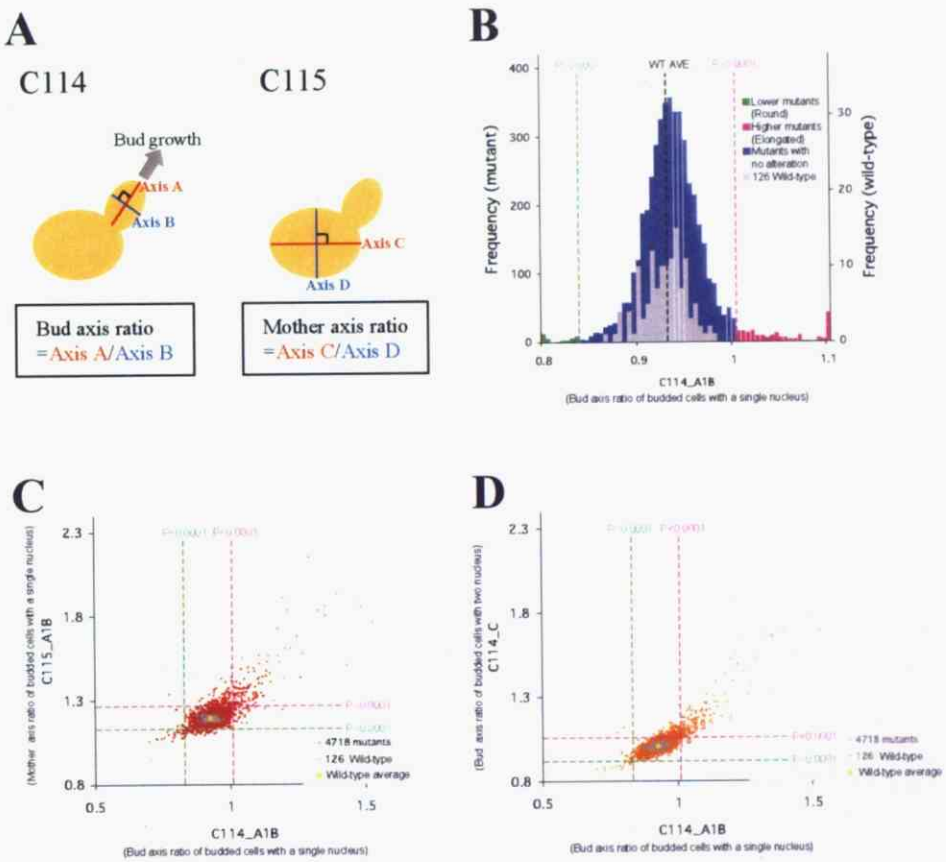

Figure 3. Quantitative morphological analysis of the bud.
(A) The definition of the parameter. An image processing program automatically recognizes the growth axis of the bud (axis A) and the axis perpendicularly crossing the axis A (axis B). The ratio of the axis A length to the axis B length corresponds to the bud axis ratio. It also recognizes the long axis of the mother cell (axis C) and the short axis perpendicularly crossing the axis C (axis D). The ratio of the axis C length to the axis D length corresponds to the mother axis ratio. (B) Distribution of 126 repetitives of wild-type and all the 4,718 yeast mutants that are able to grow in rich media. The distribution of average of bud axis ratio of budded cells with a single nucleus (C114_A1B) is shown. (C) Correlation between bud axis ratio of budded cells with a single nucleus (C114_A1B) and mother axis ratio of budded cells with a single nucleus (C115_A1B). (D) Correlation between bud axis ratio of budded cells with a single nucleus (C114_A1B) and bud axis ratio of budded cells with two nuclei (C114_C). Green and magenta lines show lower and upper threshold, respectively.

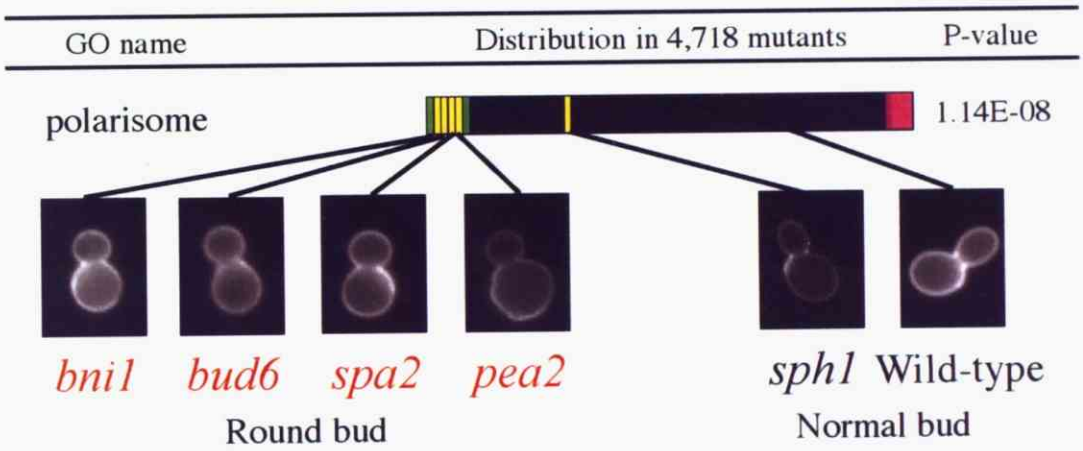

Figure 4. Polarisome mutants are enriched in round bud mutants.
4,718 mutants are sorted by bud axis ratio. Mutants that exhibit significant abnormality are shown in green (round bud mutants) and magenta (elongated but mutants), respectively. The positions of polarisome mutants (annotated by Gene Ontology consortium) carrying disruption of the indicated gene are indicated with yellow lines.

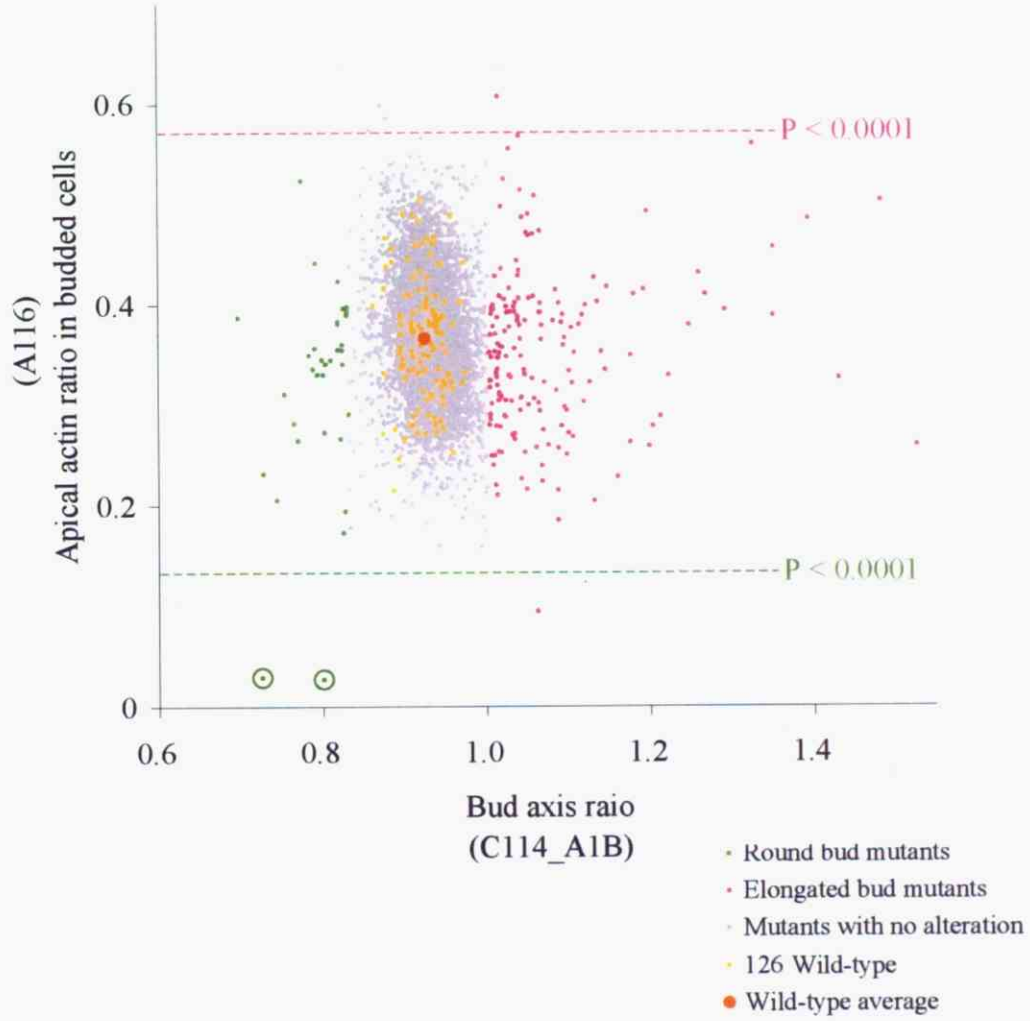

Figure 5. Classification of round bud mutants by actin localization.
Correlation between bud axis ratio of cells with a single nucleus (C114_A1B) and apical actin ratio in budded cells (A116). Mutants that have significant abnormality in C114_A1B are shown in green (round bud mutants) and magenta (elongated bud mutants). Green circles show mutants that have significant abnormality in A116. Green and magenta lines show lower and upper threshold, respectively.

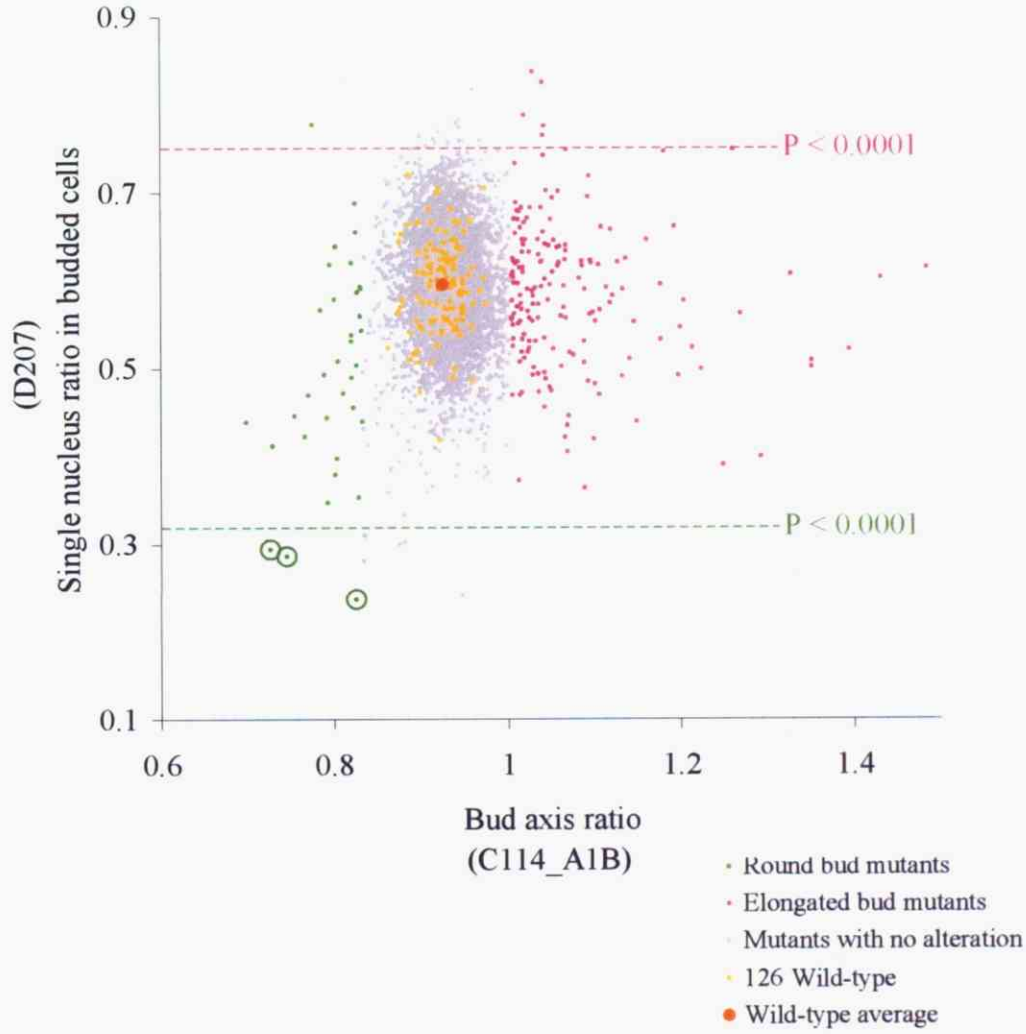

Figure 6. Classification of round bud mutants by state of nucleus.
Correlation between bud axis ratio of cells with a single nucleus (C114_A1B) and single nucleus ratio in budded cells (D207). Mutants that have significant abnormality in C114_A1B are shown in green (round bud mutants) and magenta (elongated bud mutants). Green circles show mutants that have significant abnormality in D207. Green and magenta lines show lower and upper threshold, respectively.

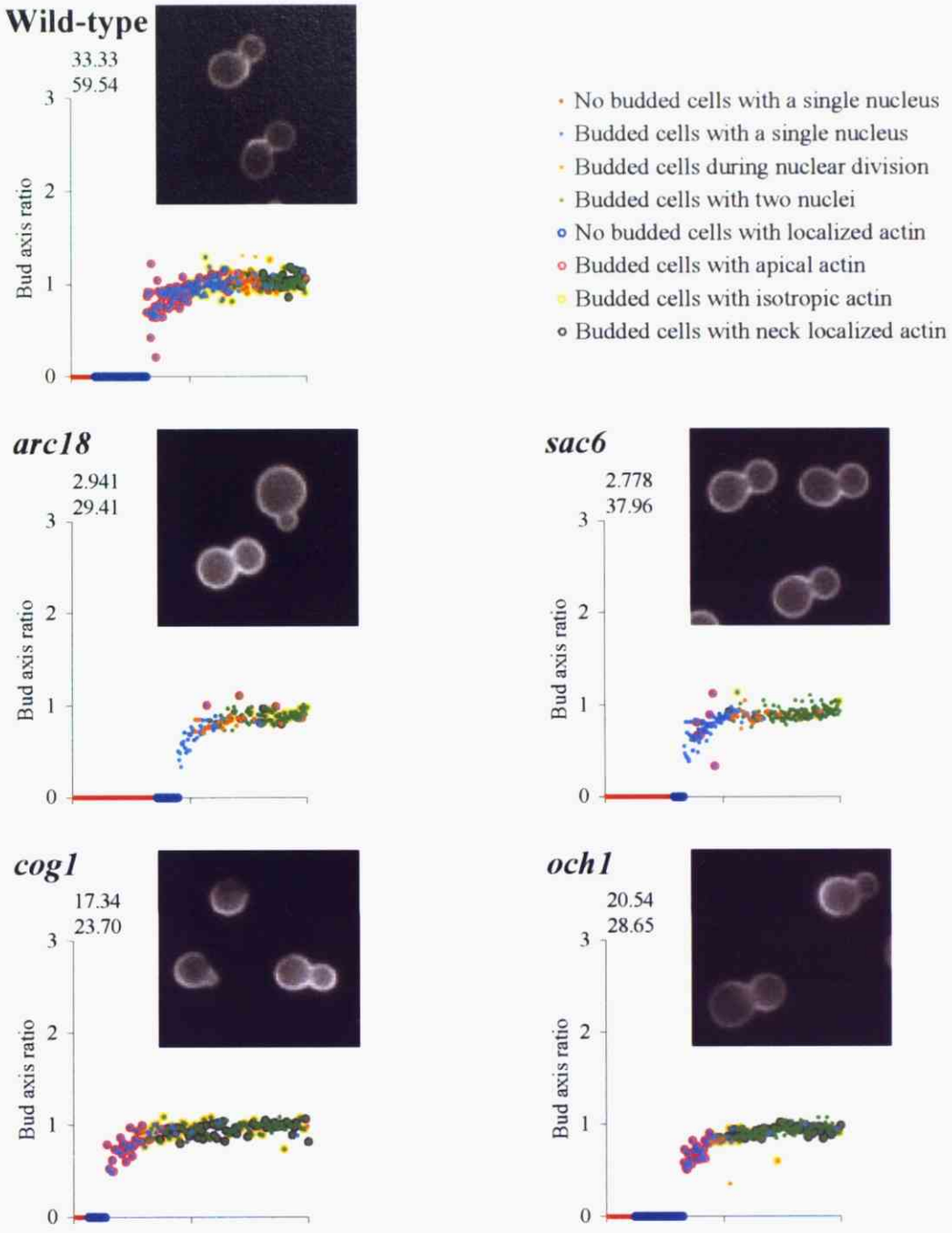

Figure 7. Bud, actin and nuclear state of round bud mutants.
Relationship between bud growth and bud morphology, actin localization, number and position of nucleus. The horizontal axis is displayed in the rank order of ratio of bud size to mother cell size of each cell ($n > 200$, normalized to become same width). Dots and circles are colorized with state of nucleus and actin distribution of the cells, respectively. Red, sky blue, orange and green dots show no budded cells with a single nucleus, budded cells with a single nucleus in mother cell, budded cells during nuclear division and budded cells with two nuclei in the mother cell and bud, respectively. Blue, pink, yellow and black circles show no budded cells with localized actin, budded cells with apical actin, budded cells with isotropic actin and budded cells with neck-localized actin, respectively. The numerals in graph show values of A116 (upper) and D207 (lower).

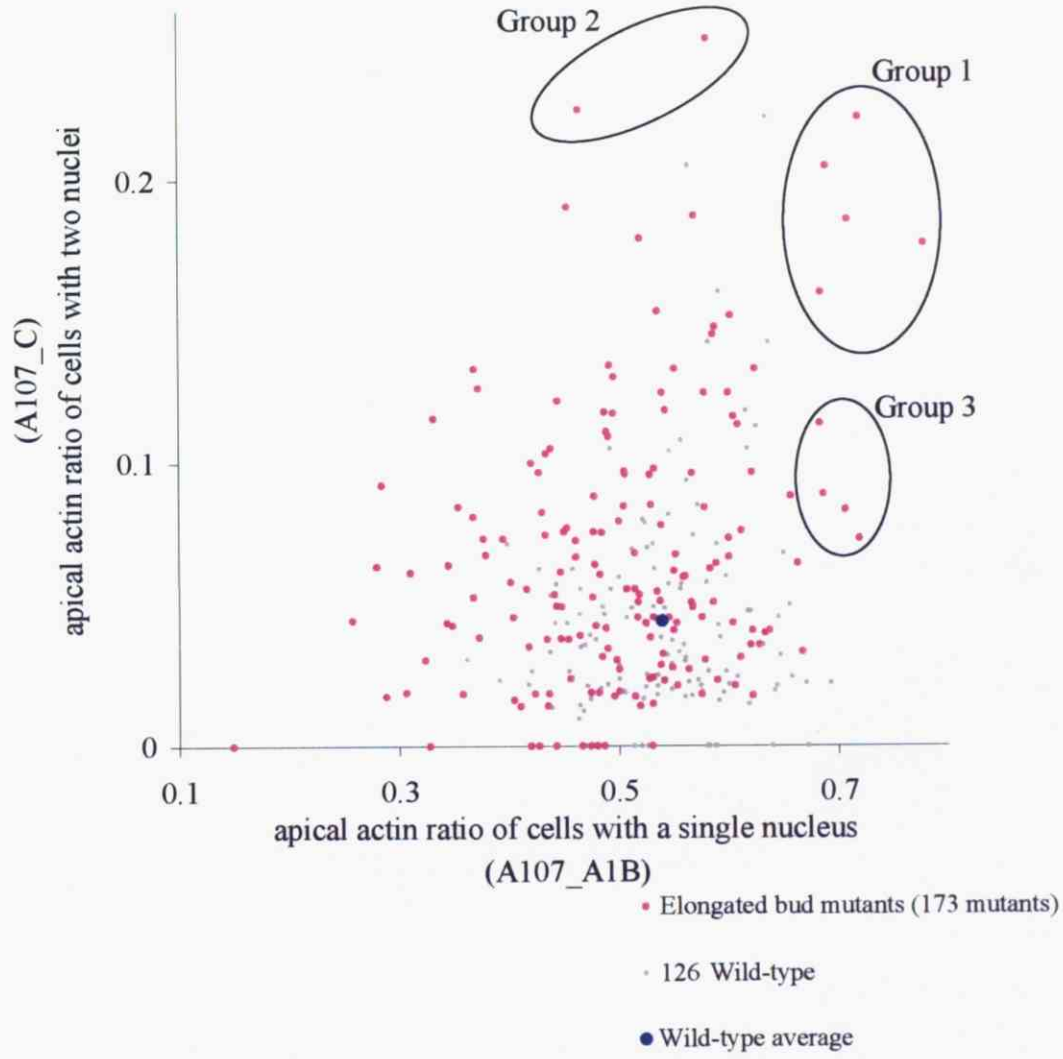

Figure 8. Classification of elongated bud mutants by actin localization.
The values of apical actin ratio of budded cells with a single nucleus in mother (A107_A1B) and that of budded cells with two nuclei in mother and bud (A107_C) are plotted. Elongated bud mutants are shown in magenta. Black circles correspond to each group of the mutants.

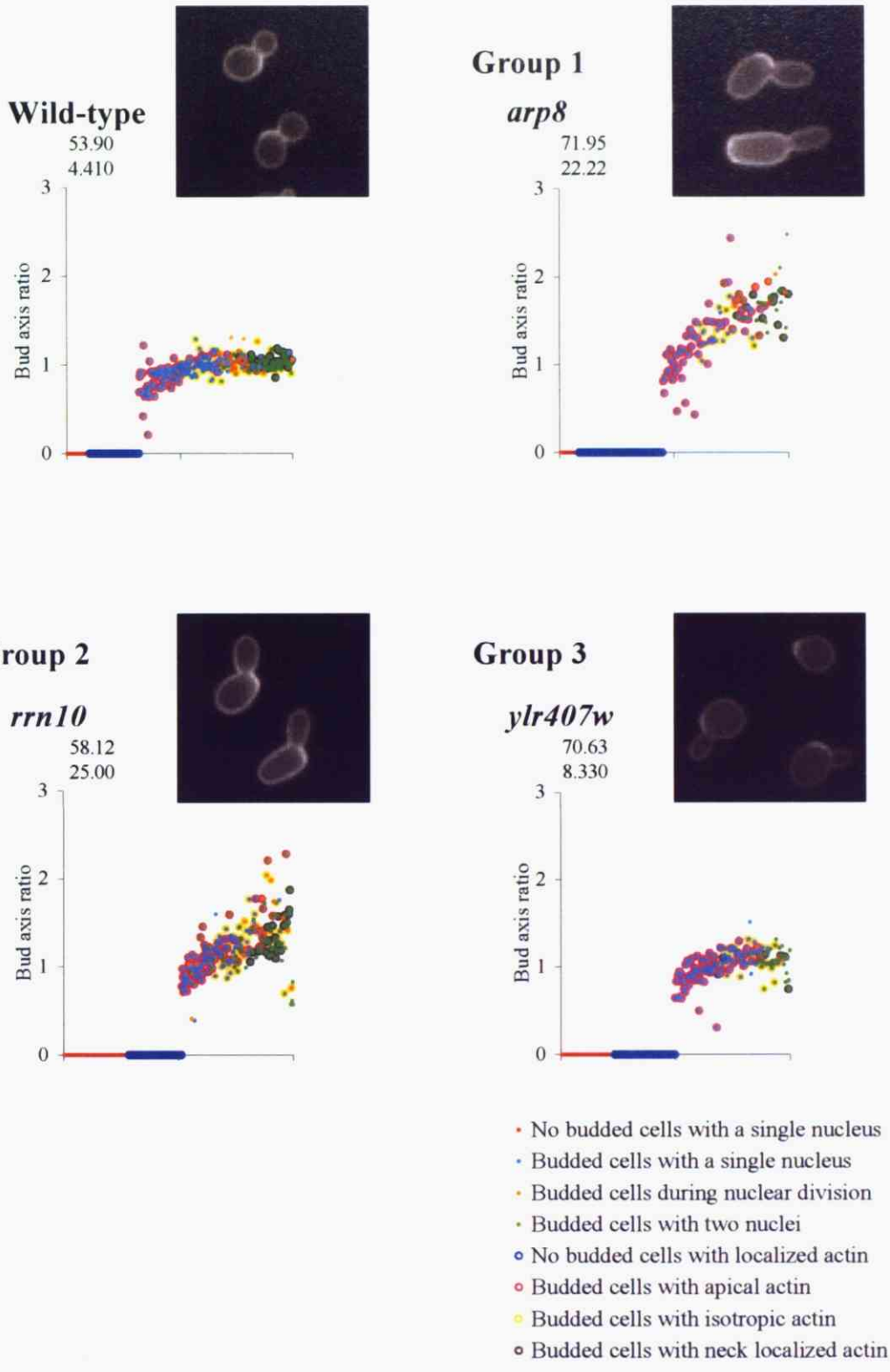

Figure 9. Bud, actin and nuclear state of elongated bud mutants.
These graphs use the same format as Figure 8. One mutants from each group classified in Figure9 is shown as an example. The numerals in graph show apical actin ratio of budded cells with a single nucleus in mother (A107_A1B, upper) and two nuclei in mother and bud (A107_C, lower).

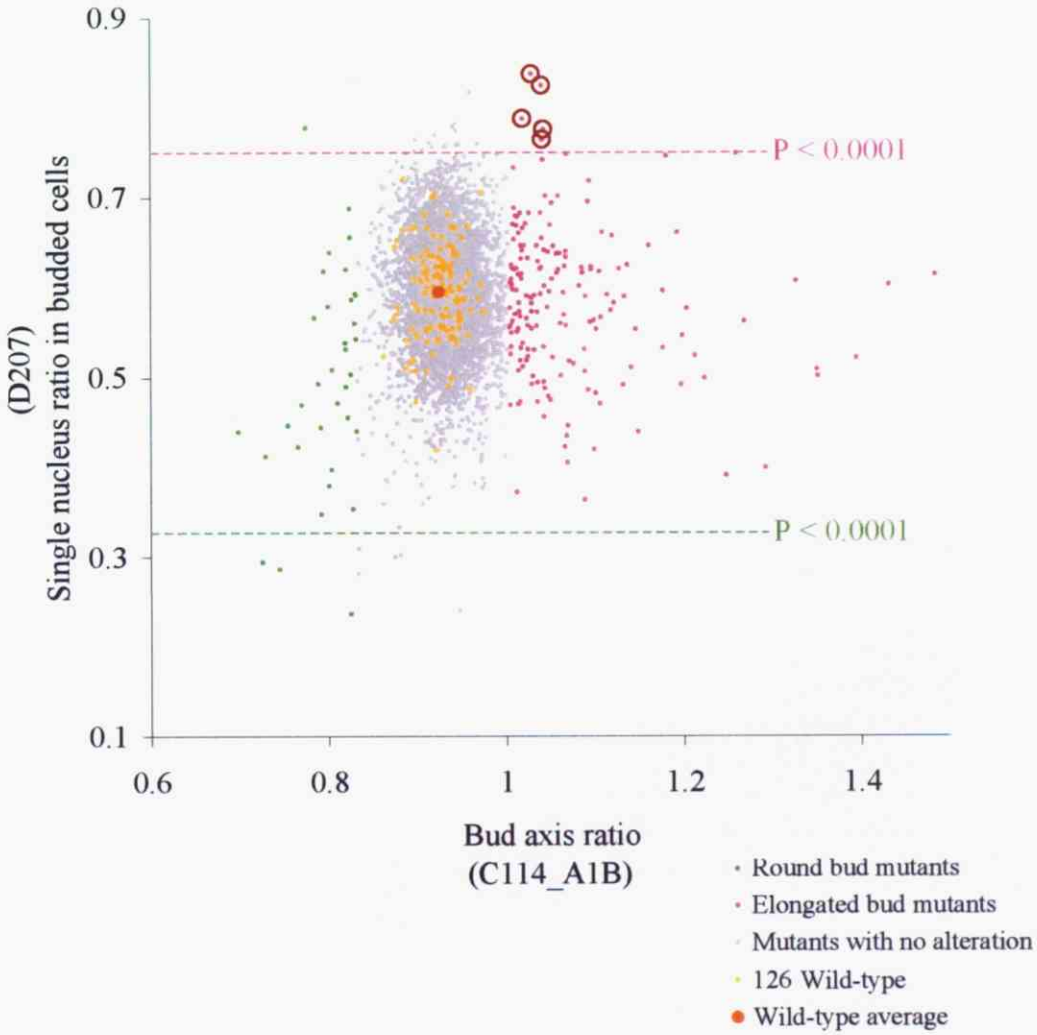

Figure 10. Classification of elongated bud mutants by state of nucleus.
Correlation between bud axis ratio of cells with a single nucleus (C114_A1B) and single nucleus ratio in budded cells (D207). Mutants that have significant abnormality in C114_A1B are shown in green (round bud mutants) and magenta (elongated bud mutants). Magenta circles show mutants that have significant abnormality in D207. Green and magenta lines show lower and upper threshold, respectively.

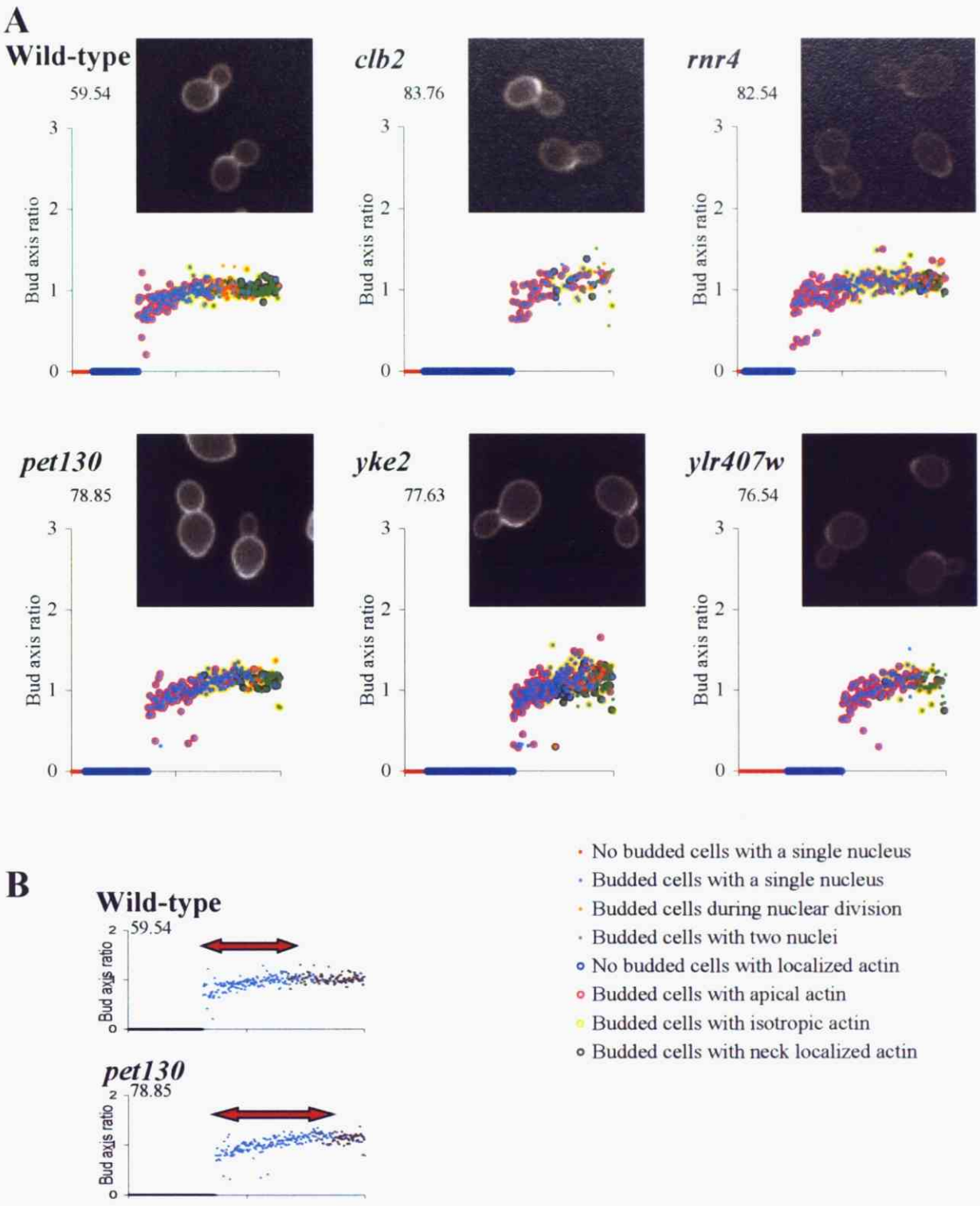

Figure 11. Elongated bud mutants that show nuclear division delay.
(A) These graphs use the same format as Figure 8. The numerals in graph show D207 values. (B) This graph shows only the state of nucleus. Sky blue dots show budded cells with a single nucleus in mother cell. Gray dots show other states of nucleus. A red arrow indicates the period before nuclear division. The numerals in graph show ratio of budded cells with a single nucleus in mother (D207).

Table 1. List of mutants with abnormal bud morphology.

Mutants	GO annotation
Round mutants (35 mutants)	
gas1	cell wall organization and biogenesis*
arc18	actin filament organization*
bni1	actin filament organization*
och1	protein amino acid N-linked glycosylation
cax4	protein amino acid N-linked glycosylation*
snc2	endocytosis*
bud6	actin filament organization*
pap2	mitotic sister chromatid cohesion*
dal5	allantoate transport
mms22	double-strand break repair
vps15	protein amino acid phosphorylation*
anp1	protein amino acid N-linked glycosylation
spa2	actin filament organization*
ybl094c	biological process unknown
sac6	endocytosis*
gat2	transcription
ggc1	mitochondrial genome maintenance*
ylr111w	biological process unknown
vma7	vacuolar acidification
rho4	actin filament organization*
tpm1	actin filament organization*
imp2'	DNA repair*
yps7	biological process unknown
sla1	cell wall organization and biogenesis*
pea2	actin filament organization*
ost4	protein amino acid N-linked glycosylation
cog1	intra-Golgi transport*

Mutants	GO annotation
ccw12	cell wall organization and biogenesis*
huf2	biological process unknown
she4	actin cytoskeleton organization and biogenesis*
ost3	protein complex assembly*
yps6	biological process unknown
ypl185w	biological process unknown
pep3	vacuole fusion, non-autophagic*
cap1	barbed-end actin filament capping
Elongated mutants (173 mutants)	
apq12	mRNA export from nucleus
cdc10	cell wall organization and biogenesis*
tif3	translational initiation
arp5	protein targeting to vacuole*
ies6	metabolism
spt20	histone acetylation*
arp8	biological process unknown
spt10	chromatin remodeling*
rpl13b	protein biosynthesis
gon7	cell wall mannoprotein biosynthesis*
scp160	chromosome segregation*
shp1	sporulation (sensu Fungi)*
elm1	protein amino acid phosphorylation*
vps75	protein targeting to vacuole
ydr532c	biological process unknown
akr1	endocytosis*
ylr358c	biological process unknown
prp18	nuclear mRNA splicing, via spliceosome*
dia4	aerobic respiration*

Mutants	GO annotation
yjl075c	biological process unknown
pro1	proline biosynthesis
rrn10	transcription from RNA polymerase I promoter
nup133	mRNA export from nucleus*
rpp1a	translational elongation*
deg1	RNA processing
scs2	chromatin silencing at telomere*
iwr1	meiosis
ngg1	histone acetylation*
ydr241w	biological process unknown
bfr1	meiosis*
brr1	spliceosome assembly
npl6	protein import into nucleus
rps12	protein biosynthesis
bud32	protein amino acid phosphorylation*
kel1	cellular morphogenesis*
rpl27a	protein biosynthesis
spt7	protein complex assembly*
shs1	establishment of cell polarity (sensu Fungi)*
sit4	cell wall organization and biogenesis*
dhh1	deadenylylation-dependent decapping*
hpr1	mRNA export from nucleus*
ylr021w	biological process unknown
ymr031w-a	biological process unknown
hop2	synapsis
ada2	histone acetylation*
snt309	nuclear mRNA splicing, via spliceosome
yer119c-a	biological process unknown
gin4	protein amino acid phosphorylation*

Table 1.

Mutants	GO annotation
sac3	mRNA export from nucleus*
dia2	invasive growth (sensu Saccharomyces)*
uaf30	transcription from RNA polymerase I promoter
bud27	bud site selection
nup170	mRNA export from nucleus*
taf14	chromatin remodeling*
ylr322w	biological process unknown
dbp7	35S primary transcript processing*
dbf2	protein amino acid phosphorylation*
ctf8	mitotic sister chromatid cohesion
trm9	response to stress*
ist3	nuclear mRNA splicing, via spliceosome*
sto1	nuclear mRNA splicing, via spliceosome*
hxk2	replicative cell aging*
bud13	nuclear mRNA splicing, via spliceosome*
vps64	protein targeting to vacuole*
lsm7	nuclear mRNA splicing, via spliceosome*
spt21	regulation of transcription from RNA polymerase II promoter
sse1	protein folding
rpa49	transcription from RNA polymerase I promoter
ccr4	regulation of transcription from RNA polymerase II promoter*
ymr185w	biological process unknown
sgf73	histone acetylation
ykl121w	biological process unknown
yel059w	biological process unknown
gcn5	histone acetylation*
fur4	uracil transport
sfp1	transcription from RNA polymerase III promoter*
fre8	metal ion homeostasis

Table 1.

Mutants	GO annotation
nup84	mRNA export from nucleus*
ybr134w	biological process unknown
gpm2	biological process unknown
hmo1	plasmid maintenance
set5	biological process unknown
hnt3	biological process unknown
rpb9	transcription from RNA polymerase II promoter
ynl171c	biological process unknown
asf1	DNA damage response, signal transduction resulting in induction of apoptosis
rsc2	chromatin remodeling*
ssz1	protein biosynthesis
yke2	protein folding*
adk1	nucleotide metabolism*
htz1	regulation of transcription from RNA polymerase II promoter*
rpb4	mRNA export from nucleus*
ylr407w	biological process unknown
tma64	biological process unknown
rnr4	DNA replication
yaf9	chromatin remodeling*
alf1	post-chaperonin tubulin folding pathway*
syg1	signal transduction
vps71	protein targeting to vacuole*
paf1	DNA recombination*
ydl151c	biological process unknown
ctf4	DNA repair*
tif4631	translational initiation
met7	one-carbon compound metabolism
gis2	intracellular signaling cascade

Table 1.

Mutants	GO annotation
srb5	transcription from RNA polymerase II promoter
rpn10	ubiquitin-dependent protein catabolism
kem1	35S primary transcript processing*
clb2	G2/M transition of mitotic cell cycle*
rps27b	protein biosynthesis
spc72	mitotic sister chromatid segregation*
ygr071c	biological process unknown
bnr1	actin filament organization*
bud4	bud site selection*
kap123	protein import into nucleus
faa3	lipid metabolism*
srv2	cytoskeleton organization and biogenesis*
ecm30	cell wall organization and biogenesis
pro2	proline biosynthesis
rcy1	endocytosis
rps0b	protein biosynthesis*
swc5	chromatin remodeling
swc3	chromatin remodeling*
psp1	biological process unknown
bul2	protein monoubiquitination*
pet130	biological process unknown
yll033w	sporulation (sensu Fungi)
rpl2b	protein biosynthesis
lem3	phospholipid translocation*
rad27	DNA repair*
pho2	transcription*
atg17	autophagy
ctk2	protein amino acid phosphorylation*
bar1	protein catabolism

Table 1.

Mutants	GO annotation
mir1	phosphate transport
rpl35a	protein biosynthesis
cdc40	nuclear mRNA splicing, via spliceosome*
tps1	response to stress*
air1	mRNA export from nucleus*
ynr004w	biological process unknown
leo1	transcription from RNA polymerase II promoter*
ylr334c	biological process unknown
soy1	biological process unknown
grr1	G1/S transition of mitotic cell cycle*
hap4	transcription*
rad54	chromatin remodeling*
rnr1	DNA replication
ydl068w	biological process unknown
pho85	protein amino acid phosphorylation*
rpl14a	protein biosynthesis
elg1	DNA replication*
ies4	biological process unknown
fen1	vesicle-mediated transport*
pho5	phosphate metabolism*
ldb18	biological process unknown
cik1	meiosis*
ydr049w	biological process unknown
rsc1	chromatin remodeling*
ayr1	phosphatidic acid biosynthesis
qri8	ER-associated protein catabolism*
ymr031c	biological process unknown
nam7	mRNA catabolism*
rrm3	mitochondrial genome maintenance*

Table 1.

Mutants	GO annotation
ubc13	protein monoubiquitination*
ktr4	protein amino acid N-linked glycosylation
hhf1	chromatin assembly or disassembly
fus3	protein amino acid phosphorylation*
vps72	protein targeting to vacuole*
cdc73	DNA recombination*
ygr160w	biological process unknown
cla4	protein amino acid phosphorylation*
rtt106	negative regulation of DNA transposition
rga1	actin filament organization*

All mentioned here are sited from *Saccharomyces* Genome Database (http:// genome-www.Stanford.edu/Saccharomyces/).

* means the gene with two or more GO annotation.

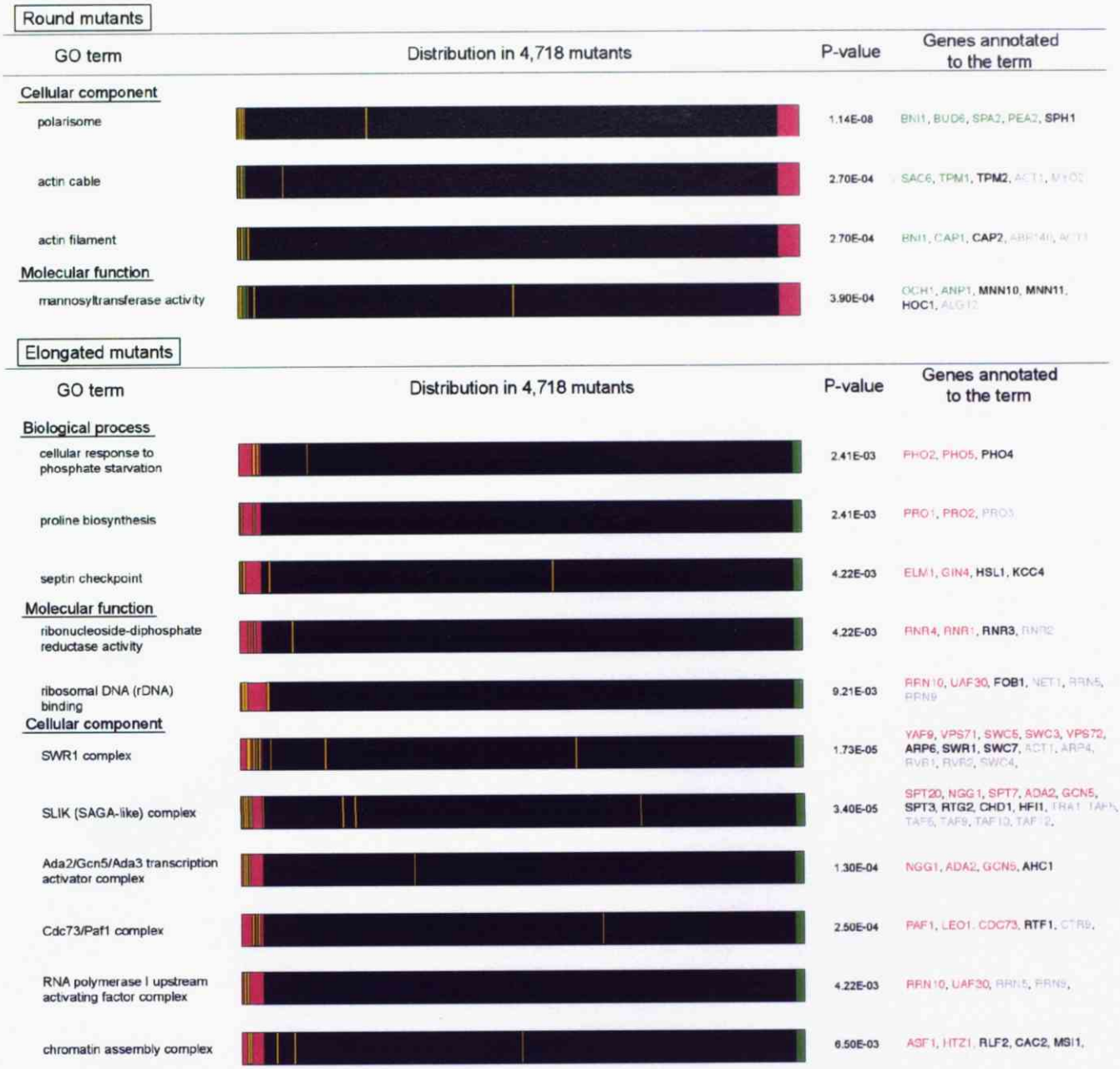

Table 2. List of GO terms with strong correlation and high phenotypic similarity in Molecular function, Biological process and Cellular component.

4,718 mutants are sorted by bud axis ratio. Mutants that exhibit significant abnormality are shown in red (elongated bud mutants) and green (round bud mutants). Positions of mutants carrying disruption of the indicated gene in the right column are shown in yellow lines. Essential genes are shown in gray.

Table 3. Yeast strains used in this study.

Strain	Genotype	Source
BY4741	MATa *his3Δ1 leu2Δ0 met15Δ0 ura3Δ0*	EUROSCARF
ykl121w	*BY4741 ykl121w::Kan^r*	EUROSCARF
bud13	*BY4741 bud13::Kan^r*	EUROSCARF
ylr407w	*BY4741 ylr407w::Kan^r*	EUROSCARF
swc3	*BY4741 swc3::Kan^r*	EUROSCARF
clb2	*BY4741 clb2::Kan^r*	EUROSCARF
rnr4	*BY4741 rnr4::Kan^r*	EUROSCARF
pet130	*BY4741 pet130::Kan^r*	EUROSCARF
yke2	*BY4741 yke2::Kan^r*	EUROSCARF

All strain used in this study was obtained from European *Saccharomyces cerevisiae* Archive for Functional Analysis (EUROSCARF).

Table 4. List of primers used in this study.

Name	Sequence	Source
HK/kanB	CTGCAGCGAGGAGCCGTAAT	A
MW/ykl121w	ATTTTGAAAACAACTAACAGGCAAC	this study
MW/bud13	CTGTTAGGTTCTTCGAGAACACATT	this study
MW/ylr407w	ATGAGTGATAGAGGCATTGAACTTT	this study
MW/swc3	TTCGACCGGACCTTTTTAAGTACGA	this study
MW/clb2	GAATTGATACTTCTGAAAAGCGAAA	this study
MW/mr4	TTCAATGTTCCTAAAGTTTCATTCC	this study
MW/pet130	CAAAACGAAAGGTAGGATTCACTTA	this study
MW/yke2	TGAAAATTTTACTGTAGTGCGATGA	this study

Reference: A; Kanai H., unpublished.